Наносистеми, наноматеріали, нанотехнології
Nanosistemi, Nanomateriali, Nanotehnologii
2023, т. 21, № 4, сс. 843–858

PACS numbers: 07.07.Df, 68.37.Lp, 68.37.Ps, 77.55.F-, 81.16.-c, 83.80.Mc, 92.60.jk

Capacitive Humidity Sensors Based on Nanocellulose Obtained from Various Non-Wood Raw Materials

Vladyslav Lapshuda, Viktoriia Koval, Valerii Barbash, Mykhailo Dusheiko, and Olga Yashchenko

National Technical University of Ukraine
'Igor Sikorsky Kyiv Polytechnic Institute',
37, Peremohy Prosp.,
UA-03056 Kyiv, Ukraine

Humidity sensors are fabricated on base of nanocellulose (NC) using different initial raw materials (reed stalks or wheat straw) and by means of different extraction methods (TEMPO-oxidation or acid hydrolysis). In addition, nanocomposites from NC with addition of polyvinyl alcohol (PVA) are used to improve the mechanical characteristics of nanocellulose films obtained by hydrolysis method. The static and dynamic characteristics of humidity sensors are measured, and their sensitivity, response, hysteresis, response and recovery times, as well as short- and long-term stability are determined. The influence of initial materials and extraction methods for NC, as well as amount of humidity-sensitive material, on device parameters is established. The dependence of sensor sensitivity on the NC mass is determined. In particular, it is shown that NC sensors made of reed have higher sensitivity, but worse stability and dynamic parameters compared to sensors made of wheat. The maximum value of sensitivity (0.204 $(\%\,\mathrm{RH})^{-1}$) is observed for sensor based on the NC film obtained of reed by TEMPO-oxidation method. Minimal signal fluctuations (10%) during continuous operation for 1 h are observed for NC sensors obtained of wheat by the hydrolysis technique. Improved response time and recovery time (7 s and 6 s) are available for NC sensors obtained of wheat by the TEMPO-oxidation method. As shown, the NC film mass of 0.3 mg is favourable for all sensors. The effect of test signal frequency is as follows: improving of sensitivity occurs at 100 Hz, and of all other parameters—at 1000 Hz.

Створено сенсори вологости на основі наноцелюлози (НЦ) із використанням різної сировини (стебел очерету чи то соломи пшениці) та різними методами (ТЕМПО-окисненням і кислотною гідролізою). Також було використано НЦ-нанокомпозити з додаванням полівінілового спирту (ПВС) для поліпшення механічних характеристик плівок наноцелюлози, одержаних методом гідролізи. Було виміряно статичні та динамічні характе-

ристики сенсорів вологости та визначено їхні чутливість, відгук, гістерезу, час відгуку та відновлення, а також коротко- та довгочасну стабільність. Встановлено вплив природи сировини та методу синтези НЦ, а також кількости вологочутливого матеріялу на поверхні сенсора на його параметри. Визначено залежність чутливости сенсорів від маси НЦ. Зокрема, було показано, що сенсори, виготовлені на основі НЦ з очерету, мають вищу чутливість, однак гіршу стабільність і динамічні параметри порівняно з сенсорами, виготовленими на основі НЦ з пшениці. Максимальна чутливість (0,204 $(\%\,\mathrm{RH})^{-1}$) спостерігається для сенсора на основі плівки НЦ, одержаної з очерету методом ТЕМПО-окиснення. Мінімальні флюктуації сиґналу (10%) сенсора під час неперервної роботи упродовж 1 год спостерігалися для сенсорів, одержаних методом гідролізи з пшениці. Поліпшені час відгуку та час відновлення (7 с і 6 с) мають місце для сенсорів на основі НЦ, одержаної з пшениці методом ТЕМПО-окиснення. Показано, що найліпші параметри спостерігаються для сенсорів з масою вологочутливої плівки у 0,3 мг. Вплив частоти тестового сиґналу був наступний: поліпшення чутливости має місце на частоті у 100 Гц, а всіх інших параметрів — на 1000 Гц.

Key words: nanocellulose, humidity sensors, biodegradable sensors.

Ключові слова: наноцелюлоза, сенсори вологости, біорозкладні сенсори.

(Received 7 April, 2023; in revised form, 10 April, 2023)

1. INTRODUCTION

The control of the relative humidity (RH) of surrounding environment is needed in many areas of modern human life: agriculture, medicine, food industry, electronics industry, automotive industry and everyday life. For example, it needs to keep the relative humidity at 80–90% for plants' growth in agriculture. The food industry needs to keep a high level of RH in order to avoid of food mass loss during storage. In addition, it is known that RH at 1% is strongly recommended in microelectronic industry for preventing corrosion of terminals. In medicine, the control of RH is used for a few purposes: control of air conditions in the hospitals (department of surgery, incubators for newborns, *etc.*) and sweat or breath monitoring in sport training and diagnose of some illness (sleep apnoea, cardiovascular diseases, asthma, *etc.*). Besides, it is important to keep RH at the level of 50–60% for human well-being [1–5].

There are several types of humidity sensors converting directly relative humidity into an electrical signal: resistive sensors, capacitive sensors, thermal conductometric sensors, and oscillator-based sensors. Other types of sensors include cold mirror and a fibre optic humidity sensor that operate with an optical signal [6–8]. Among them, capacitive-type sensors have huge advantages: low response

and recovery times, small size, possibility of to be integrated into an IC's with a processing part. This type of sensor converts value of RH into a capacitance that can be measured [8].

The popular materials for humidity-sensitive layers in capacitive sensors are nanoporous silica/silica oxide, metal oxides (ZnO, Al_2O_3, $BaTiO_3$, In_2O_3, *etc.*) [9–12], polymers (PI, PDMS, PVA, *etc.*) [13–16], carbon nanomaterials (nanorods, graphene) [15, 17, 18]. Today, the newest trend in electronics is the use of biodegradable materials (nanocellulose, chitin, *etc.*). Such materials are very promising for both single-use devices and short-life devices, because they do not need to be disposed. Instead of intent recycling, these devices simply rot in the soil and do not pollute the environment.

Nanocellulose (NC) is a natural polymer that can be obtained from wood and non-wood plant raw materials. This material has good humidity absorption characteristics due to its developed surface and the presence of free hydroxyl groups in cellulose molecules [4, 19]. It is possible to obtain nanocellulose by the method of oxidation in a TEMPO solution (TEMPO-oxidation method), or by the method of acid hydrolysis [20, 21]. Currently, NC is made of reed [4, 22, 23], wheat [4], miscanthus [19], kenaf [4] and hemp [24]. However, there is a lack of complete information concerning the influence of different types of raw materials and methods of NC extraction from them, as well as the amount of NC on the sensor surface on the characteristics of humidity sensors.

Therefore, the purpose of this paper is to study the influence of the initial material (reed and wheat) and extraction technique of NC (TEMPO-oxidation and acid hydrolysis), as well as its amount (0.3–3 mg) on sensor characteristics.

2. EXPERIMENTAL PART

Preparation of Nanocellulose. For the transformation of the plant material into nanocellulose, we first obtained cellulose from wheat straw and reed stalks using an environmentally friendly method of organosolv delignification of raw materials, which is carried out at low temperature and in a relatively short time, and then nanocellulose was extracted from it by oxidation and hydrolysis methods. Briefly, the process of nanocellulose obtaining from wheat straw and reed stalks can be represented by such three stages. At the first stage, the chopped stalks of the raw material were delignified for 90 min at a temperature of 97 ± 2°C in a solution containing glacial acetic acid and 35% hydrogen peroxide in a volume ratio of 7:3, when the ratio of liquid to solid was equal 10:1. At the second stage, alkaline treatment of cellulose was carried out at a temperature 97 ± 2°C with a 7% NaOH solution at a liquid-to-solid ratio of

12:1 for 90 min. At the third stage, nanocellulose was extracted from the obtained cellulose by hydrolysis or oxidation methods.

The acid hydrolysis of the cellulose was carried out in 43% sulfuric acids at the liquid to solid ratio 10:1, at temperatures of 60°C for 60 min, to obtain a suspension of hydrolysed nanocellulose. Then this suspension rinsed with distilled water three times by means of centrifugation at 4000 rev/min and subsequent dialysis, until it reached pH 7. To form a homogeneous suspension, nanocellulose was treated with ultrasound at 22 kHz for 60 min [20].

To obtain nanocellulose by means of the oxidation of 2,2,6,6-tetramethylpiperidine-1-oxyl (TEMPO), the prepared cellulose was transferred into a beaker, filled with distilled water, and the obtained aqueous cellulose suspension was mixed with sodium bromide 16 wt.% and TEMPO 1.6 wt.%. To uniformly impregnate cellulose suspension with these reagents, we used sonication in the ultrasound disintegrator UZDN-A (SELMI) at 22 kHz for 5 min. Then a sodium hypochlorite solution was poured into suspension, wherein the pH was controlled within 10–11 by adding solution of sodium hydroxide 0.5 M NaOH. The duration of the TEMPO-oxidation was 24 hours. To stop the TEMPO-oxidation process, we added ethanol C_2H_5OH and 0.5 M HCl to the slurry until the pH reached 7. Then the slurry was centrifuged three times at 3000 rpm for 30 min each, and the ultrasonic treatment of the TEMPO-oxidized nanocellulose suspension was carried out for 10 min [21].

Sensor Fabrication. Sensor fabrication process consists of the following steps (Fig. 1). The first operation was the metal film deposition on sitall substrate. The deposition was done using RF sputtering technique with the next parameters: pressure in the chamber $5 \cdot 10^{-3}$ mm Hg, operating voltage of 600 V and operating current of 1 A. As a result, two-layered Ti/Ni film of 0.25 μm thick was obtained. The second step was the photolithography process in order to obtain the interdigital electrodes from continuous Ti/Ni film. After that, plate with transducers was cut down into separate samples. Electrical wires to the electrodes were soldered. The last operation was the deposition of a humidity-sensitive film top on the surface of transducers by drop-casting method using NC hydrogel. Then nanocellulose was dried in the thermal chamber at 50°C for 1 hour. This step was repeated several times in order to obtain NC of different thickness. We used 4 kinds of pure nanocellulose and 2 kinds of NC-based composites: nanocellulose, produced from reed and wheat using TEMPO (NC–RT and NC–WT, accordingly) and hydrolysis (NC–RG and NC–WG, accordingly), and mixture of NC and PVA (1:1), obtained by hydrolysis. We used composites because RG and WG NC-films have weak adhesion to the surface and are capable of cracking. PVA was used to improve adhesion and plastic-

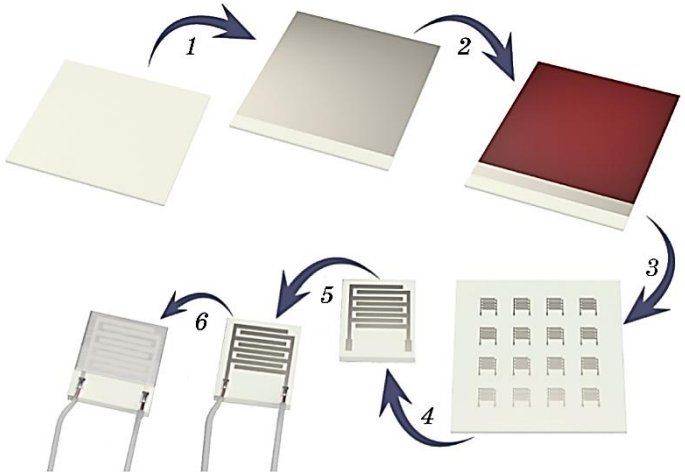

Fig. 1. The manufacturing process of humidity sensors based on nanocellulose: deposition of a Ti/Ni film on sitall substrate (*1*); coating and drying of photoresist (*2*); photolithography process (*3*); cutting the plate into separate sensors (*4*); soldering wires to sensor electrodes (*5*); drop-casting of NC sensitive layer (*6*).

ity of NC films.

Characterization Technique. Hygrostats based on saturated salt solutions were used to measure the characteristics of humidity sensors. According to Raoult's law, a saturated solution of salt will generate a stable relative humidity in the near-surface air. We used the following salts that generated the certain values of RH: LiCl—12%, $MgCl_2$—33%, NaBr—60%, NaCl—75%, KCl—85%, H_2O—98%. An EZODO HT-390 thermohygrometer was used to control humidity in hygrostats. The P-5030 RLC meter was used to measure sensor parameters at frequencies of 100 Hz and 1 kHz. Investigation of sensors was done by measuring of static (response, sensitivity, hysteresis) and dynamic characteristics (repeatability, response time and recovery time, short- and long-term stability). In particular, the value of response and sensitivity was determined from the adsorption curve, that is, the dependence of capacitance on the level of RH, when it increases from 12 to 85%. The response was defined as the difference between the maximum and minimum capacitance values in the studied RH range. Since the adsorption curve of sensors has an exponential dependence, the sensitivity was determined as a power of exponent in equation of approximating curve. To study the hysteresis of obtained sensors, the adsorption and desorption curves were measured in one cycle (RH changed from 12 to 98% and from 98 to 12%, respectively). The value of hysteresis was determined due the next equation:

$$H = \pm \frac{\Delta C_{\max}}{C_{\max} - C_{\min}} \cdot 100\%,$$

where $\Delta C_{\max}$ is the maximum difference of capacitance on the adsorption–desorption curves at the same RH, $(C_{\max} - C_{\min})$ is sensor response in the whole range of RH. The repeatability of sensor signals was investigated by 6-times cycling between RH levels of 12 and 60%. The deviation of capacitance values between adjacent cycles was determined. The response time and recovery time were measured during change in relative humidity from 12 to 60% and from 60 to 12%, when the value of the sensor signal reached 90% or 10% of the initial value accordingly. The short-term stability of the sensors was evaluated during their continuous operation for 1 h at constant relative humidity (12 and 60%). The short-term stability is presented as signal fluctuation near the average value. Long-term stability (ageing) was determined after 6–12 months of storage, after that the relative change of device sensitivity was calculated.

3. RESULTS AND DISCUSSION

Structure and Chemical Composition of NC. To analyse the size of nanocellulose particles obtained by TEMPO-oxidation and acid hydrolysis of organosolv celluloses from reed stalks and wheat straw, we used TEM (Fig. 2) and AFM (Fig. 3).

As can be seen in Fig. 2 and Fig. 3, nanoparticles with a diameter of 5–45 nm (NC–RT), 12–43 nm (NC–RG), 6–13 nm (NC–WT) and 10–30 nm (NC–WG) were obtained.

Sensitivity of NC Humidity Sensors. The principle operation of capacitive humidity sensors is to increase of capacitance when humid-

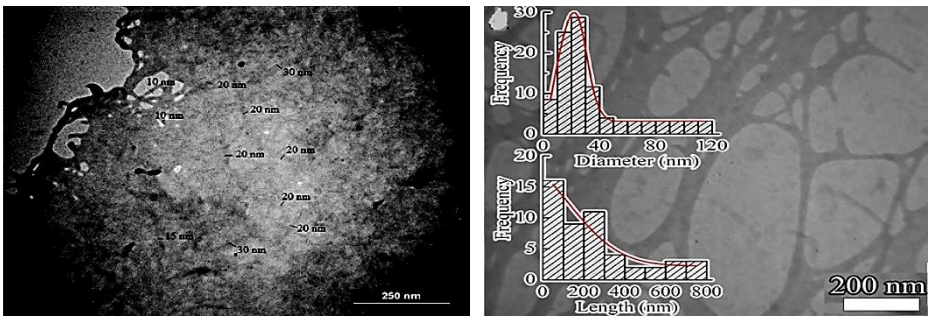

a *b*

Fig. 2. TEM images of nanocellulose prepared by hydrolysis of organosolv wheat straw cellulose (*a*) and by TEMPO-oxidation of organosolv reed cellulose (*b*).

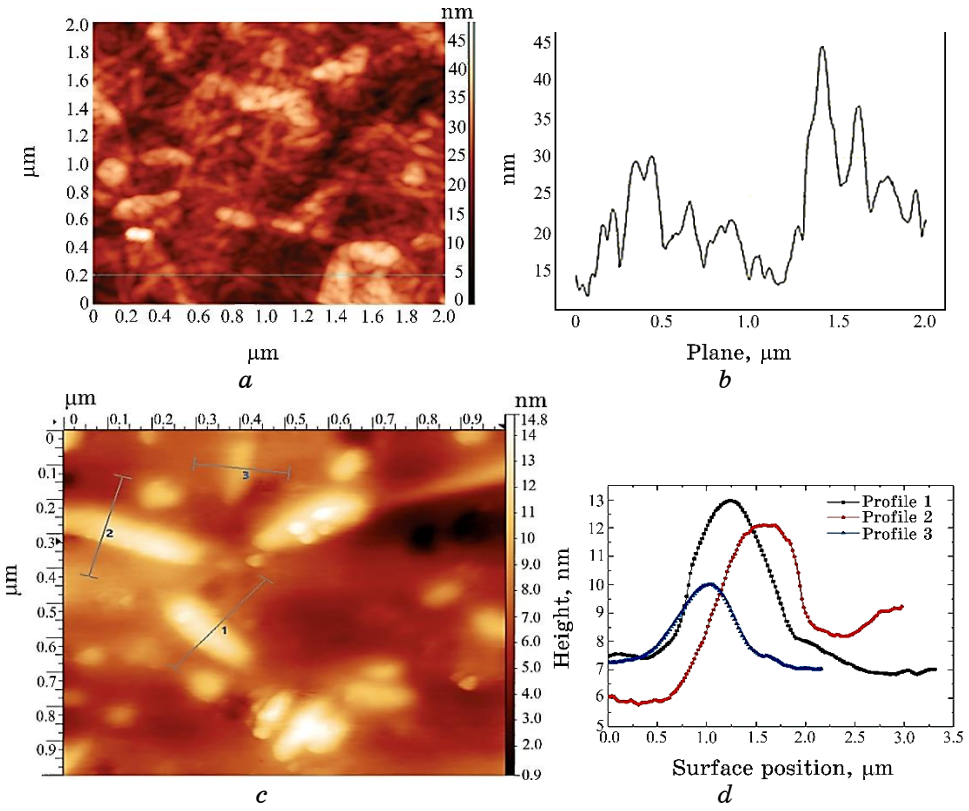

Fig. 3. AFM images of nanocellulose prepared by hydrolysis of organosolv reed cellulose (*a*) and by TEMPO-oxidation of organosolv wheat straw cellulose (*b*).

ity increases in the environment. This phenomenon is observed because the dielectric constant of nanocellulose increases due to adsorbed water molecules. It was shown that capacitance of the device increases with increasing of RH exponentially (adsorption curve) (Fig. 4, *a*). The mechanism of water adsorption is explained by the presence of a large number of free hydroxyl groups in nanocellulose macromolecules. Besides, well-developed surface of NC allows obtaining sensors with a significant response.

Comparison of different NC synthesis methods for the same initial material and mass of NC film (0.3 mg) revealed that sensor sensitivity is higher for TEMPO-oxidation method than for acid hydrolysis one: 0.204 $(\%\,\mathrm{RH})^{-1}$ *vs.* 0.190 $(\%\,\mathrm{RH})^{-1}$ for reed and 0.168 $(\%\,\mathrm{RH})^{-1}$ *vs.* 0.134 $(\%\,\mathrm{RH})^{-1}$ for wheat. In addition, it can be seen from the data in Fig. 4, *b*, regardless of synthesis method, the sensitivity of NC films obtained from reed is higher than that from wheat. This dependence is

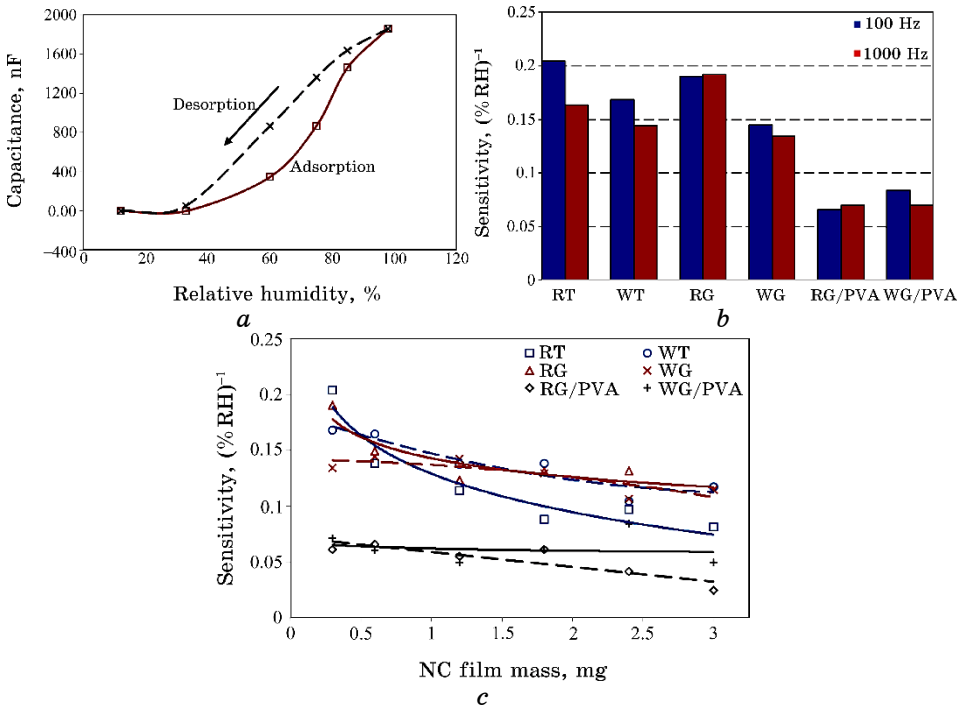

Fig. 4. Adsorption and desorption curves for NC humidity sensor (*a*), diagram of maximal sensitivity (*b*) and dependence of sensitivity on NC mass for each NC composition (*c*).

related to different diameter of nanofibers in obtained nanocellulose. We can see that the diameter of nanofibers obtained from reed is larger compared to nanofibers from wheat for both nanocellulose extraction methods. One can conclude that thicker nanofibers are able to adsorb a larger amount of humidity.

Obtained sensors can be placed according to the decrease of sensitivity in the following sequence: RT–RG–WT–WG, *i.e.*, the most preferable NC suspension for humidity sensors is RT, which provides maximum value of sensitivity. Such sequence can be explained by the different surface structure of nanocellulose nanofibers. NC particles obtained by the TEMPO-oxidation method have carboxyl groups on the surface of cellulose macromolecules (Fig. 5, *a*), which create fewer spatial complications for the penetration of water molecules to the hydroxyl groups of the 2nd and 3rd carbon atoms in neighbouring pyranose chains, than ester sulphate groups on the surface of nanocellulose obtained by acid hydrolysis (Fig. 5, *b*).

Ester sulphate groups cover a larger surface area of nanocellulose, reducing the possibility of interaction with water molecules, which de-

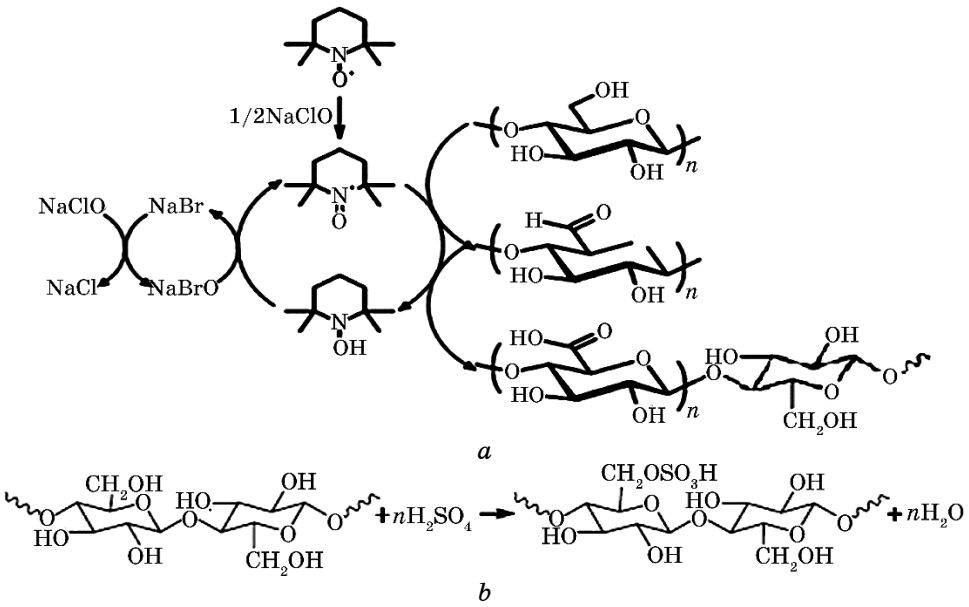

Fig. 5. Mechanism of TEMPO-oxidation (*a*) and acid hydrolysis (*b*) methods of nanocellulose obtaining.

teriorates its hydrophilicity. At the same time, the sensitivity of sensors based on PVA/NC composites is significantly lower than that of pure nanocellulose. This behaviour can be explained by the fact that PVA forms smooth films with small specific surface area.

In addition, it was established that sensitivity of humidity sensors decreases with the increase in NC mass on their surface for all types of initial materials and regardless of nanocellulose extraction techniques (Fig. 4, *c*). This behaviour is because as mass of humidity-sensitive film increases, its thickness increases too (sample area was the same). It is known, the electric field is mainly concentrated between the ends of adjacent electrodes and near of them. With increasing of NC-layer thickness, the adsorbed water is further away from the surface of electrodes and, accordingly, from the action area of electric field. It should be noted that the magnitude of device sensitivity decrease with increasing of NC mass depends on the type of initial NC suspension. For NC from reed this drop is 2 times more than for NC from wheat for both synthesis methods. The same ratio is observed for different NC extraction methods: the drop is more for TEMPO than for hydrolysis technique. Thus, the lowest influence of NC film mass on device sensitivity is observed for NC–WG (14.5%), and the highest one is for NC–RT (60%). A similar dependence is determined for composites: the drop in sensitivity with NC mass growth was much greater for

RG/PVA than for WG/PVA.

One can see that as test signal frequency increases, the device sensitivity decreases for pure cellulose and almost does not change for the composites. The decrease in device sensitivity with an increase of test signal frequency can be explained by the frequency dispersion of dielectric constant of nanocellulose: polarization rate of water molecules is lower than change rate of test signal. Therefore, water molecules do not have enough time to polarize completely, which results in the decrease of dielectric constant for nanocellulose as well as device response.

Hysteresis of NC Humidity Sensors. One can see in Fig. 6, *a* that humidity adsorption and desorption curves forms a hysteresis loop, which is due to different speeds of adsorption and desorption processes. Adsorption is an endothermic process, so it is faster than desorption, which is an exothermic process. The diagram in Fig. 6, *b* shows the average values of device hysteresis for each NC composition for two frequencies of test signal (100 and 1000 Hz). One can see that magnitude of hysteresis is affected by both the initial material and the technique of NC extracting. In particular, NC obtained from wheat provides a lower device hysteresis compared to NC obtained from reed: 22% *vs*. 32% for TEMPO-oxidation method and 20% *vs*. 25% for acid hydrolysis method. As for technique of NC extracting, there is a decrease in hysteresis when replacing TEMPO with hydrolysis: from 32% to 25% for reed and from 22% to 20% for wheat. Obtained sensors can be placed according to the decrease of hysteresis in the following sequence: RT–RG–WT–WG. That is, the most preferable NC suspension for humidity sensors is WG, which provides minimal value of hysteresis. The point is that the NC from reed has a larger fibre diameter than the NC from wheat. We can assume that the thinner NC nanofibers desorb a hu-

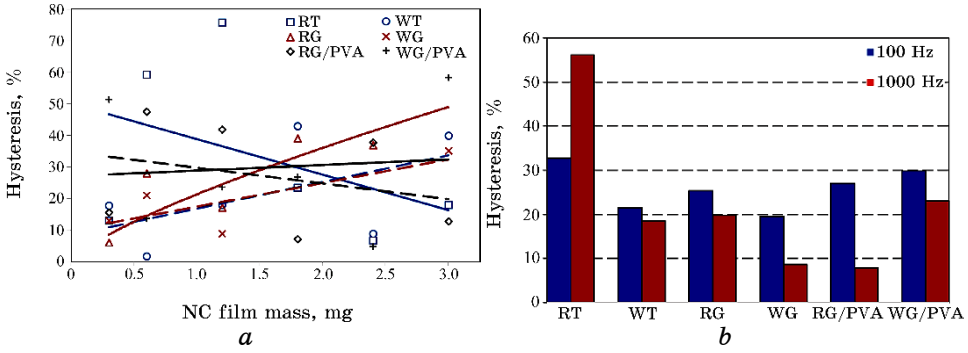

Fig. 6. Dependence of hysteresis on NC mass (*a*) and diagram of average hysteresis for each NC composition (*b*).

midity faster, which results in a smaller hysteresis value. In addition, it was determined that less hydrophilic NC, obtained by the acid hydrolysis technique, has a lower value of hysteresis compared to TEMPO-oxidation method. Adding PVA to NC, we can observe a noticeable increase in device hysteresis, which can be explained by both the effect of PVA itself and the interaction with NC.

Figure 6, *a* shows the dependence of hysteresis on NC film mass: the greater the mass of humidity-sensitive film, the greater the device hysteresis. This can be explained by the fact that desorption lasts longer from a thicker film. The frequency dependence is also clearly visible (Fig. 6, *b*): when the frequency of test signal increases, the hysteresis of obtained sensors decreases. This behaviour can be explained by the fact that certain processes, affecting hysteresis, stop to work due to their slowness at higher frequency.

Cycling of NC Humidity Sensors. The repeatability of sensor parameters was studied with a cyclic change in relative humidity from 12% to 60% and *vice versa*. As can be seen in Fig. 7, *a*, sensor repeatability depends on initial material for the synthesis of NC: nanocellulose obtained from reeds provides worse repeatability than NC from wheat (27% *vs.* 6% for the TEMPO-oxidation method and 24% *vs.* 13% for

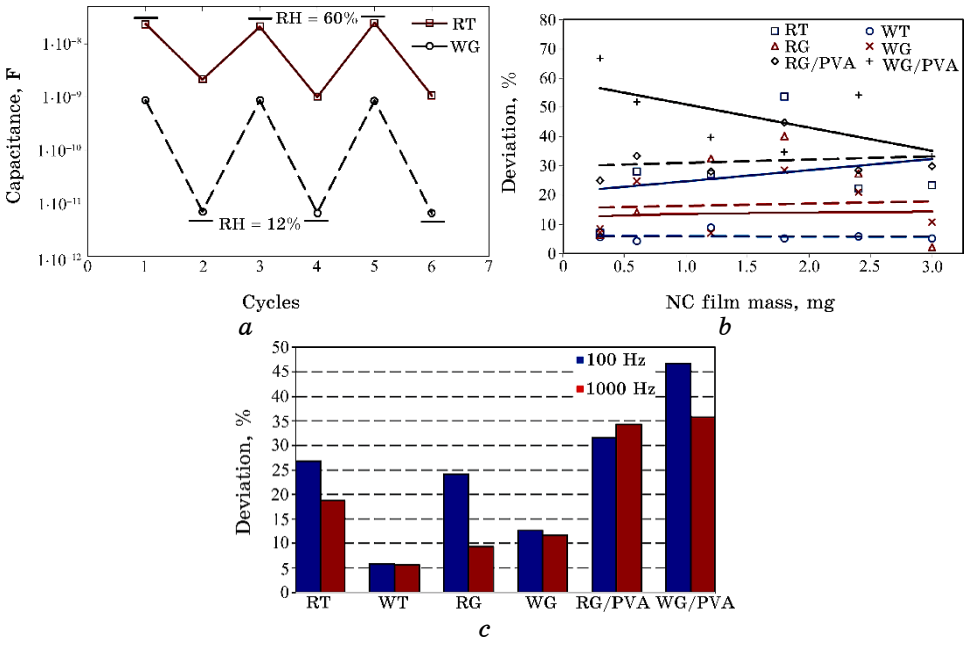

Fig. 7. Response curves for NC humidity sensor under humidity cycling (*a*), dependence of sensor signal deviation on NC mass (*b*) and diagram of average deviation for each NC composition (*c*).

the acid hydrolysis method). The most repeatable measurement results are demonstrated by sensors based on WT (the value of the deviation between cycles is 6%). This behaviour is explained by much smaller thickness of nanofibers in NC–WT compared to NC from reed. The difference in nanofibre thickness can affect the rate of adsorption–desorption processes. NC–PVA composites show an increase in instability compared to pure nanocellulose (31% and 47% for RG/PVA and WG/PVA, respectively).

Figure 7, *b* shows the influence of NC mass on the deviation of sensor signal during the cycling measurements and, namely, for the most NC solutions, including NC/PVA composites, there is no effect of mass on sensor repeatability. Besides, it was determined when the frequency of test signal increases from 100 to 1000 Hz, the value of the deviations decreases for all samples. At the same time, the most influence of signal frequency on the device deviations is observed for sensors based on NC–RT (from 27% to 19%).

Short-Term Stability of NC Humidity Sensors. Figure 8, *a* shows the change in sensor signal during 1 hour of exposure in an environment with the constant humidity (RH of 60%). Based on these

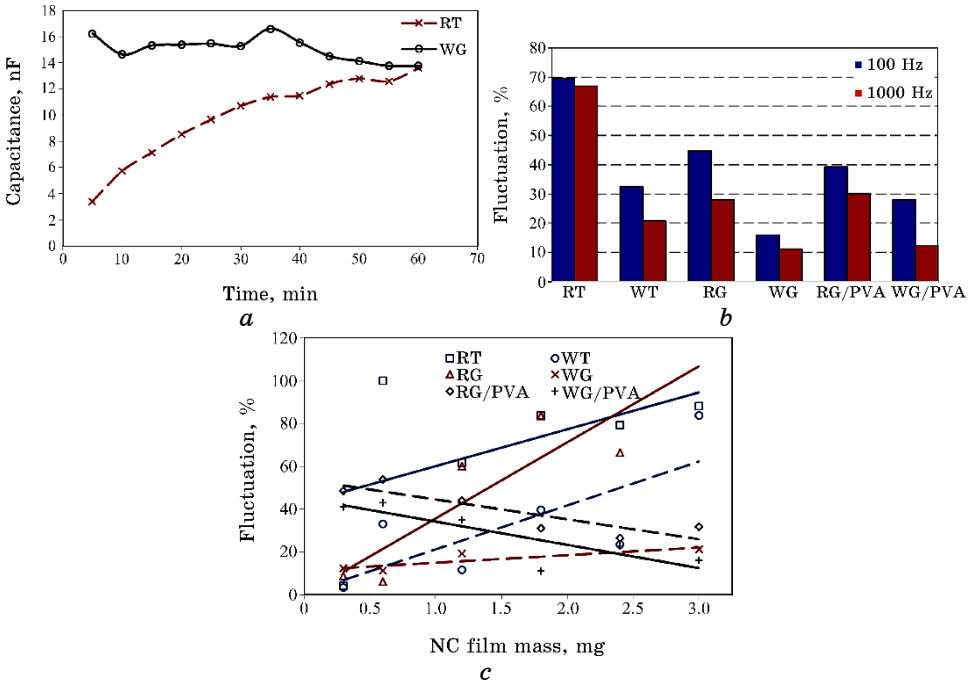

Fig. 8. Short-time stability curves for NC–RT and NC–WG sensors (*a*), diagram of average sensor signal fluctuation for each NC composition (*b*) and dependence of fluctuation on NC mass (*c*).

dependencies, the short-term stability of the devices was evaluated. There are two cases of unstable sensor behaviour: random fluctuations near the equilibrium value (for WG, WT) or a gradual increase of the signal (RT, RG) (Fig. 8, *a*). The observed random fluctuations of the signal can be due to the temporal instability of humidity absorption process by NC film because of its well-developed surface. The gradual increase of the signal means that thermodynamic equilibrium does not have enough time to be fully established. Due to the large diameter of nanofibres, process of adsorption is continued for NC–RT and NC–RG. Small size of WT and WG nanofibres allows the thermodynamic processes to occur faster.

If we compare the NC extracting techniques, we will get an improvement in device stability from 70 to 45% for reed and from 32 to 16% for wheat when comparing the TEMPO and hydrolysis methods. Obtained sensors can be placed according to the increase of short-term stability in the following sequence: RT–RG–WT–WG. That is, the most preferable NC suspension for humidity sensors is WG, which provides minimal value of signal fluctuations. At the same time, the stability of WG/PVA composites is significantly improved, and RG/PVA composites are slightly worsened in comparison with pure NC solutions that need further research. Figure 8, *a* illustrates the influence of NC film mass on signal fluctuations during these measurements. As we can see, all sensors based on pure NC show an increase in instability as the mass of humidity-sensitive film increases, while sensors made of PVA/NC composites, on the contrary, demonstrate an improvement in stability.

From Figure 9, *a* one can evaluate response and recovery speed for obtained sensors: the smaller NC mass, the shorter device response time. The minimum response time for different initial raw materials and NC extracting techniques lies within 7–27 s for pure nanocellulose and 95–280 s for NC–PVA composites. In addition,

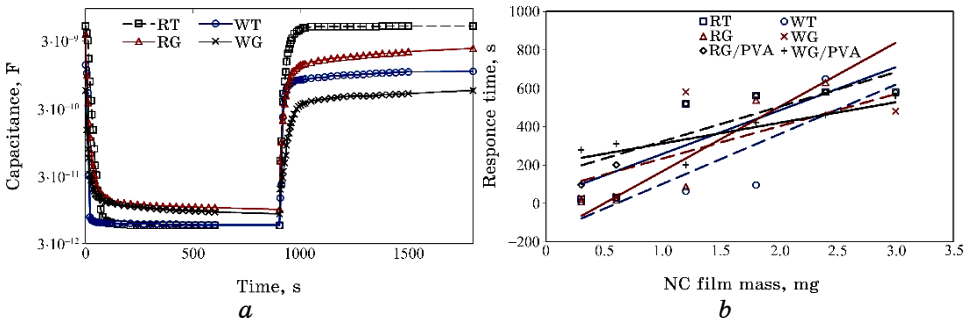

Fig. 9. Response and recovery time characteristics (*a*) and dependence of response time on NC mass for each NC compositions (*b*).

we can observe that the recovery time is less than the response time for all devices: 6–22 s for pure nanocellulose and 22–135 s for NC–PVA composites. As known, the desorption is slower process than the adsorption and, accordingly, the recovery time should be longer. Similar behaviour occurred for capacitive sensors in [19] and perhaps related to the fact that NC expands in volume during adsorption, which forms new adsorption centres and increase of response time. In addition, it was established that the response and recovery times are larger for NC–PVA composites. This behaviour can be explained by the fact that adding of PVA to NC deteriorates pore-like morphology of NC, due to which the diffusion rate of humidity in the depth and out of material slows down.

Long-Term Stability of NC Humidity Sensors. Long-term stability was investigated by measuring the capacitance of obtained sensors with a certain period (2, 6 and 12 months) and fewer than two levels of relative humidity (12 and 60%). It was established that the capacitance of all sensors decreased over time. The value of aging was estimated as the relative change in device signal between the extreme time points of the study. Since different sensors were measured during various periods, the relative change in capacitance over 1 day was calculated. For obtained sensors, the amount of aging varied from 0.23%/day to 1.24%/day. For sensors made of NC–RT and NC–WT this parameter is of 0.25%/day and 0.23%/day, which is several times less compared to the sensors based on NC–RG and NC–WG (0.73%/day and 1.24%/day, respectively). Thus, it is possible to conclude that the higher long-term stability is observed for NC obtained by TEMPO-oxidation method, regardless of initial raw material.

4. CONCLUSION

In this study, humidity sensors were made based on nanocellulose extracted from various initial raw materials (reed and wheat), using different extraction methods (TEMPO-oxidation and acid hydrolysis), with different mass of humidity-sensitive film on sensor surface (from 0.3 mg to 3.0 mg). Sensors based on PVA/NC bionanocomposite in a ratio of 1:1 were also obtained to improve the adhesion and plasticity of NC films extracted by hydrolysis.

It was shown that sensors based on NC made of reed have better response and sensitivity than those from wheat. In addition, the use of TEMPO-oxidation method provides improved sensor sensitivity compared to the acid hydrolysis method. However, short-term stability, reversibility, repeatability are significantly worse for reed compared to wheat. If high sensitivity is needed, it is advisable to use sensors from NC–RT. If it is necessary to ensure better stability

of the sensors, then it is more appropriate to use NC–WG. It was also shown that the best parameters are observed for the sensors with NC mass of 0.3–0.6 mg.

The addition of PVA significantly made better the mechanical characteristics of nanocellulose films extracted by hydrolysis method, but at the same time worsened the device parameters. Therefore, the direction of further research is the synthesis of a PVA-based nanocomposite with a lower PVA content in order to obtain a NC film with improved parameters.

REFERENCES

1. A. Yamamoto, H. Nakamoto, T. Yamaguchi, H. Sakai, M. Kaneko, S. Ohnishi, T. Nishiuma, K. Sawada, Y. Iwata, S. Osawa, K. Ono, and A. Ishikawa, *Respir. Med.*, **190**: 106675 (2021); https://doi.org/10.1016/j.rmed.2021.106675
2. H. Tai, S. Wang, Z. Duan, and Y. Jiang, *Sens. Actuators B*, **318**: 128104 (2020); https://doi.org/10.1016/j.snb.2020.128104
3. J. Wu, Y. Chen, W. Shen, Y. Wu, and J.-P. Corriou, *Ceram. Int.*, **49**, No. 2: 2204 (2023); https://doi.org/10.1016/j.ceramint.2022.09.187
4. V. Koval, V. Barbash, M. Dusheyko, V. Lapshuda, O. Yashchenko, and Y. Yakimenko, *Proc. of Symp. '2020 IEEE 10th International Conference Nanomaterials: Applications & Properties (NAP)' (Nov. 9–13, 2020)* (Sumy: SumDU), p. 1; https://doi.org/10.1109/NAP51477.2020.930959
5. H. Niu, W. Yue, Y. Li, F. Yin, S. Gao, C. Zhang, H. Kan, Z. Yao, C. Jiang, and C. Wang, *Sens. Actuators B*, **334**: 129637 (2021); https://doi.org/10.1016/j.snb.2021.129637
6. G. M. Patel, V. R. Shah, G. J. Bhatt, and P. T. Deota, *Nanosensors for Smart Manufacturing* (Eds. S. Thomas, T. A. Nguyen, M. Ahmadi, A. Farmani, and G. Yasin) (Kerala, India: Elsevier: 2021), p. 555.
7. J. Fontes, *Sensor Technology: Handbook* (Ed. John S. Wilson) (Burlington, MA, U.S.A.: Elsevier: 2005), p. 271.
8. G. Urban, *Anal. Bioanal. Chem.*, **408**, No. 21: 5667 (2016); https://doi.org/10.1007/s00216-016-9637-2
9. C. K. Chung, C. A. Ku, and Z. E. Wu, *Sens. Actuators B*, **343**: 130156 (2021); https://doi.org/10.1016/j.snb.2021.130156
10. S. Das, M. L. Rahman, P. P. Mondal, P. L. Mahapatra, and D. Saha, *Ceram. Int.*, **47**, No. 23: 33515 (2021); https://doi.org/10.1016/j.ceramint.2021.08.260
11. F. D. M. Fernandez, M. Bissannagari, and J. Kim, *Ceram. Int.*, **47**, No. 17: 24693 (2021); https://doi.org/10.1016/j.ceramint.2021.05.191
12. V. Manikandan, F. Tudorache, I. Petrila, R. S. Mane, V. Kuncser, B. Vasile, D. Morgan, S. Vigneselvan, and A. Mirzaei, *J. Magn. Magn. Mater.*, **474**: 563 (2019); https://doi.org/10.1016/j.jmmm.2018.11.072
13. S. Ali, M. A. Jameel, A. Gupta, S. J. Langford, and M. Shafiei, *Synth. Met.*, **275**: 116739 (2021); https://doi.org/10.1016/j.synthmet.2021.116739
14. I. Rahim, M. Shah, A. Khan, J. Luo, A. Zhong, M. Li, R. Ahmed, H. Li, Q. Wei, and Y. Fu, *Sens. Actuators B*, **267**: 42 (2018);

https://doi.org/10.1016/j.snb.2018.03.069
15. X. Li, W. Feng, X. Zhang, S. Lin, Y. Chen, C. Chen, S. Chen, W. Wang, and Y. Zhang, *Sens. Actuators B*, **321**: 128483 (2020); https://doi.org/10.1016/j.snb.2020.128483
16. H. Zhao, Z. Wang, Y. Li, and M. Yang, *J. Colloid Interface Sci.*, **607**: 367 (2022); https://doi.org/10.1016/j.jcis.2021.08.214
17. R. Guo, W. Tang, C. Shen, and X. Wang, *Comput. Mater. Sci.*, **111**: 289 (2016); https://doi.org/10.1016/j.commatsci.2015.09.032
18. A. Kafy, A. Akther, Md. I. R. Shishir, H. C. Kim, Y. Yun, and J. Kim, *Sens. Actuators A*, **247**: 221 (2016); https://doi.org/10.1016/j.sna.2016.05.045
19. V. Lapshuda, V. Koval, V. Barbash, M. Dusheiko, O. Yashchenko, and S. Malyuta, *Proc. of Symp. '2022 IEEE 41st International Conference on Electronics and Nanotechnology (ELNANO)' (October 10–14, 2022)* (Kyiv: Igor Sikorsky Kyiv Polytechnic Institute), p. 208; https://doi.org/10.1109/ELNANO54667.2022.9927092
20 V. Barbash and O. Yaschenko, *Novel. Nanomaterials* (Ed. K. Krishnamoorthy) (London, UK: IntechOpen: 2021); https://doi.org/10.5772/intechopen.94272
21. V. A. Barbash, O. V. Yashchenko, A. S. Gondovska, and I. M. Deykun, *Appl. Nanosci.*, **12**, No. 4: 835 (2022); https://doi.org/10.1007/s13204-021-01749-z
22. V. Koval, V. Barbash, M. Dusheyko, V. Lapshuda, O. Yashchenko, and A. Naidonov, *Proc. of Symp. '2021 IEEE 11th International Conference Nanomaterials: Applications & Properties (NAP)' (November 9–13, 2020)* (Sumy: SumDU), p. 1; https://doi.org/10.1109/NAP51885.2021.9568610
23. A. Naidonov, V. Koval, V. Barbash, M. Dusheiko, O. Yashchenko, and O. Yakymenko, *Proc. of Symp. '2022 IEEE 41st International Conference on Electronics and Nanotechnology (ELNANO)' (October 10–14, 2022)* (Kyiv: Igor Sikorsky Kyiv Polytechnic Institute), p. 292; https://doi.org/10.1109/ELNANO54667.2022.9927070
24. V. A. Barbash, O. V. Yashchenko, O. S. Yakymenko, R. M. Zakharko, and V. D. Myshak, *Cellulose*. **29**, No. 18: 8305 (2022); https://doi.org/10.1007/s10570-022-04773-6